Improving estimation of entropy production rate for run-and-tumble particle systems by high-order thermodynamic uncertainty relation

Ruicheng Bao and Zhonghuai Hou*

Department of Chemical Physics & Hefei National Laboratory for Physical Sciences at Microscales, iChEM, University of Science and Technology of China, Hefei, Anhui 230026, China

(Received 29 November 2022; revised 16 January 2023; accepted 30 January 2023; published 10 February 2023)

Entropy production plays an important role in the regulation and stability of active matter systems, and its rate quantifies the nonequilibrium nature of these systems. However, entropy production is hard to experimentally estimate even in some simple active systems like molecular motors or bacteria, which may be modeled by the run-and-tumble particle (RTP), a representative model in the study of active matters. Here we resolve this problem for an asymmetric RTP in one dimension, first constructing a finite-time thermodynamic uncertainty relation (TUR) for a RTP, which works well in the short observation time regime for entropy production estimation. Nevertheless, when the activity dominates, i.e., the RTP is far from equilibrium, the lower bound for entropy production from TUR turns out to be trivial. We address this issue by introducing a recently proposed high-order thermodynamic uncertainty relation (HTUR), in which the cumulant generating function of current serves as a key ingredient. To exploit the HTUR, we adopt a method to analytically obtain the cumulant generating function of the current we study, with no need to explicitly know the time-dependent probability distribution. The HTUR is demonstrated to be able to estimate the steady state energy dissipation rate accurately because the cumulant generating function covers higher-order statistics of the current, including rare and large fluctuations besides its variance. Compared to the conventional TUR, the HTUR could give significantly improved estimation of energy dissipation, which can work well even in the far from equilibrium regime. We also provide a strategy based on the improved bound to estimate the entropy production from a moderate amount of trajectory data for experimental feasibility.

DOI: 10.1103/PhysRevE.107.024112

I. INTRODUCTION

Active matter systems consist of self-propelled particles which can perform persistent random motion through consuming energy from the environment and converting it into a nonequilibrium drive [1–5]. In the past two decades, active matter has attracted a surge of interest in the field of statistical and biological physics, because it may appropriately model living things like bacteria or flocking birds, which are far from equilibrium [2–13]. See [1] for a good review. The three most commonly used active matter models are the active Brownian particle (ABP) model [3,14,15], the active Ornstein-Uhlenbeck particles (AOUP) model [16,17], and the run-and-tumble particle (RTP) model [2,18]. ABP, AOUP, and RTP are all characterized by active forces with exponential correlations imposed on them, and all exhibit some nontrivial behaviors compared to their passive counterparts consequently even at the single-particle level [19]. For example, an active particle (ABP, AOUP, or RTP) trapped in a confined potential can reach a non-Boltzmann and non-Gaussian stationary state [16,20,21], and the probability density of a RTP or a AOUP confined in a box could concentrate near the spatial boundaries [16,22].

The entropy production plays a central role in active matter systems, quantifying the heat dissipation to environment in a steady state; in other words, quantifying the thermodynamic cost to maintain a nonequilibrium steady state for some time. However, measuring the entropy production of these systems directly in experiments is quite challenging because the temperature changes from dissipation are very small and usually elusive in the noisy environment [23]. A possible solution to this issue is the Harada-Sasa relation, which quantitatively connects the entropy production rate with the violation of the fluctuation-dissipation relation [24,25]. However, it is necessary to measure the whole frequency spectrum of the focused degree of freedom in order to use this relation, requiring a lot of statistics.

Recently, a fundamental inequality called the thermodynamic uncertainty relation (TUR) was built for general stationary Markov processes, demonstrating a tradeoff relation between precision of an arbitrary current j_τ (ratio between its squared mean and variance) and the total entropy production rate $\dot{\Sigma}$ [26–31]:

$$\frac{2k_B\langle j_\tau\rangle^2}{\mathrm{Var}(j_\tau)} \leqslant \dot{\Sigma}\tau, \tag{1}$$

where τ is the observation time of the current j_τ (from now on, we set $k_B = 1$ for notation brevity, rendering entropy dimensionless). On top of that, TUR signifies that a lower bound

*hzhlj@ustc.edu.cn

for the steady state entropy production can be established in terms of the first and second moments of any currents, which has the potential to serve as a technique to estimate entropy production only from a moderate amount of experimentally accessible trajectory data [23,32–34]. Nonetheless, the estimation from TUR is usually not accurate since the lower bound is not guaranteed to be tight in general. For instance, it has been demonstrated that TURs for general biochemical oscillations are far from tight in several important models like circadian clock and Brusselator [35]. For that reason, the accurate estimation of entropy production from available data in active matter systems is still an important open problem.

In the present work, we analytically study one of the minimal models of active matter, the RTP model, providing some useful strategies to estimate the entropy production rate of a RTP only from trajectories data obtainable from direct experimental observations. To begin, we built a finite-time TUR for this model, showing that the lower bound of entropy production given by the TUR serves as a good estimator in the short observation time limit. Nevertheless, very high temporal resolution is needed to keep the estimation robust when the activity is large. To address this, we build a tighter lower bound of entropy production as a new estimator by incorporating the effect of large and rare fluctuations. This new estimator is based on the recently proposed high-order thermodynamic uncertainty relation (HTUR) [36–38], which is robust when the RTP is arbitrarily far from equilibrium and the observation time is not short. The key quantity of the HTUR is the cumulant generating function (CGF) of the current of interest. To exploit the HTUR, we provide a novel approach to analytically calculate the CGF directly from the Fokker-Planck equations of the system. In consequence, the HTUR bound can be directly evaluated through our exact expression of the CGF. We also propose an experimentally practical strategy to get better estimation of entropy production than conventional TUR since it may not be possible to obtain the CGF in experiment. Our work provides some insight on the HTUR, which may find further applications in other active matter systems.

The rest of the paper is organized as follows. In Sec. II, we introduce the asymmetric RTP model. In Sec. III, a finite-time TUR is constructed analytically for this model, and the transport efficiency which shows the TUR's performance in estimating entropy production is evaluated under different observation times and activities. In Sec. IV, the HTUR for the RTP is derived, which is utilized to significantly improve the estimation of entropy production; this is followed by Sec. V with conclusions and outlook.

II. MODEL

Throughout this work, we consider an asymmetric one-dimensional RTP model with diffusion. In this model, the position of a single RTP is described by the Langevin equation (the mobility μ is set to be 1)

$$\frac{dx}{dt} = v\sigma(t) + \sqrt{2D}\xi(t), \tag{2}$$

where $D = T\mu = T$ is the diffusion constant, v is a constant drift velocity, $\xi(t)$ is the Gaussian white noise with zero mean $\langle\xi(t)\rangle = 0$ and delta-function correlation $\langle\xi(t)\xi(s)\rangle = \delta(t-s)$, and $\sigma(t) = \pm 1$ refers to a dichotomous telegraphic noise that switches from the run state to the tumble state at rate γ_r and at rate γ_l conversely. Note that $\sigma(t)$ is a colored noise whose stationary autocorrelation function is given by (see Appendix A for proof)

$$\langle\sigma(t)\sigma(s)\rangle = \frac{4\gamma_r\gamma_l}{(\gamma_r+\gamma_l)^2}e^{-(\gamma_r+\gamma_l)|t-s|} + \left(\frac{\gamma_r-\gamma_l}{\gamma_r+\gamma_l}\right)^2. \tag{3}$$

The corresponding Fokker-Planck equation of Eq. (2) reads

$$\frac{\partial p_r(x,t)}{\partial t} = -\frac{\partial j_r(x,t)}{\partial x} - \gamma_r p_r(x,t) + \gamma_l p_l(x,t), \tag{4}$$

$$\frac{\partial p_l(x,t)}{\partial t} = -\frac{\partial j_l(x,t)}{\partial x} + \gamma_r p_r(x,t) - \gamma_l p_l(x,t), \tag{5}$$

where the probability currents $j_{r,l}(x,t)$ are defined as

$$j_r(x,t) = [v - D\partial_x]p_r(x,t),$$
$$j_l(x,t) = [-v - D\partial_x]p_l(x,t),$$

and $p_r(x,t)$ $[p_l(x,t)]$ denotes the probability of finding a particle with velocity v $(-v)$ at position x and time t. Without loss of generality, we assume $\gamma_l > \gamma_r \geqslant 0$ so that the RTP would move along the same direction as the drift velocity v on average. To assure ergodicity, the RTP is set to be confined in a one-dimensional ring whose circumference is L, i.e., $x \in [0, L)$, so that the stationary state distribution is the uniform distribution $p^{st}(x) = \lim_{t\to\infty} p(x,t) = 1/L$. Further, the stationary distributions of the particle being in run state and tumble state are $p_r^{st}(x) = \gamma_l/(\gamma_l+\gamma_r)L$ and $p_l^{st}(x) = \gamma_r/(\gamma_l+\gamma_r)L$ respectively. However, we claim that for natural boundary condition the scheme to estimate dissipation in this paper still works in the large time limit. This can be understood by noticing that the natural boundary condition is effectively the periodic boundary condition with $L \to \infty$ for one-dimensional systems, and the entropy production rate in the large time limit and its estimator in this work are irrelevant to the system size L (see Appendix B). A schematic illustration of our model is given in Fig. 1. Very recently, Ro *et al.* experimentally studied the entropy production of a four-state run-and-tumble particle jumping along a ring, which is analogous to our model [39].

We would like to explain why we study the RTP with asymmetric transition rates between the run state and the tumble state. Molecular motors and *Escherichia coli* in nature usually exhibit directed motion. To better model this directed motion, one should consider asymmetric transition rates instead of symmetric transition rates in which case $\gamma_r = \gamma_l = \gamma$. In the symmetric case, the RTP will not display directed movement because the mean displacement $\langle x(\tau)\rangle_{x_0} - x_0$ always vanishes in the large time limit whatever the initial position x_0 is, i.e., $\langle x(\tau)\rangle_{x_0} = x_0$, just like the unbiased random walk. Here, $\langle x(\tau)\rangle_{x_0}$ is the mean position of the particle at time $t = \tau$ with the initial position at $t = 0$ being given by x_0.

III. FINITE-TIME THERMODYNAMIC UNCERTAINTY RELATION FOR A RUN-AND-TUMBLE PARTICLE

To start, we show the validity of the conventional TUR and its limitation for the estimation of energy dissipation in our

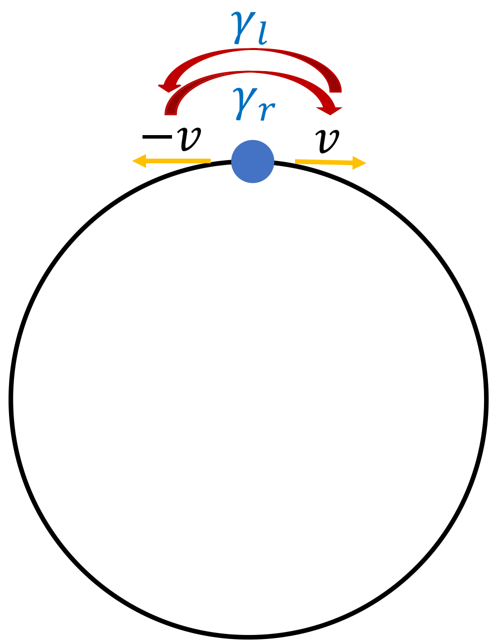

FIG. 1. An illustration of a run-and-tumble particle moving along a one-dimensional ring whose circumference is L.

model. Below, we construct a TUR and use it to estimate the steady state entropy production rate. To study the TUR, we consider a fluctuating generalized current defined as

$$j_\tau = \int_{x(0)}^{x(\tau)} w(x) \circ \dot{x}(t) dt, \tag{6}$$

where $w(x)$ is a differentiable weight function and $\circ$ denotes the Stratonovich product. We choose $w(x) = 1$ so that the resulting current is a physically relevant quantity, i.e., the displacement during the finite observation time τ. Note that the choice of mean particle displacement as the focused current is aimed to assure experimentally easy accessibility. In the stationary state, the mean value of this current $x_\tau \equiv x(\tau) - x(0) = \int_0^\tau \dot{x}(t)dt$ can be readily obtained as

$$\langle x_\tau \rangle = \int_0^\tau \langle \dot{x} \rangle dt = v \int_0^\tau \langle \sigma(t) \rangle dt = \frac{\gamma_l - \gamma_r}{\gamma_l + \gamma_r} v\tau, \tag{7}$$

and its variance in the steady state can also be computed as (see Appendix B for derivations)

$$\mathrm{Var}(x_\tau) = D_{\mathrm{eff}}\tau - \frac{8\gamma_l\gamma_r v^2}{(\gamma_l + \gamma_r)^4}[1 - e^{-(\gamma_l+\gamma_r)\tau}],$$
$$D_{\mathrm{eff}} \equiv \frac{8\gamma_l\gamma_r v^2}{(\gamma_l + \gamma_r)^3} + 2D. \tag{8}$$

Note that the variance can be calculated via the noise correlation (3), or through the moment equations method introduced in Appendix B. Since the displacement is nothing but the accumulation of instantaneous velocity during τ, $x(\tau)$ in our spatially periodic model is the same as its counterpart in the model with natural boundary condition. Equipped with expressions of the mean and variance, an estimator of the steady state mean entropy production during an observation interval τ may be obtained according to the conventional TUR:

$$\Sigma_{\mathrm{TUR}}^\tau = \frac{2\langle x_\tau \rangle^2}{\mathrm{Var}(x_\tau)}$$
$$= \frac{2\left(\gamma_l^2 - \gamma_r^2\right)^2 v^2\tau}{D_{\mathrm{eff}}(\gamma_l + \gamma_r)^4 - \frac{8\gamma_l\gamma_r v^2[1-e^{-(\gamma_l+\gamma_r)\tau}]}{\tau}} \leqslant \langle \Sigma_\tau \rangle, \tag{9}$$

which provides a lower bound of the steady state entropy production. Below, the steady state mean entropy production is calculated exactly by stochastic thermodynamics [40], so that Eq. (9) can be easily verified, i.e.,

$$\langle \Sigma_\tau \rangle = \tau \left(\int_0^L \frac{j_r^{st}(x)^2}{Dp_r^{st}(x)} dx + \int_0^L \frac{j_l^{st}(x)^2}{Dp_l^{st}(x)} dx \right)$$
$$+ \tau \int_0^L dx \left[\gamma_r p_r^{st}(x) - \gamma_l p_l^{st}(x) \right] \ln \frac{\gamma_r p_r^{st}(x)}{\gamma_l p_l^{st}(x)}$$
$$= \frac{v^2\tau}{D} \left(\frac{\gamma_l}{\gamma_r + \gamma_l} + \frac{\gamma_r}{\gamma_r + \gamma_l} \right) = \frac{v^2\tau}{D}, \tag{10}$$

where, in the second line, the relation $\gamma_r p_r^{st}(x) - \gamma_l p_l^{st}(x) = 0$ was used. The expression for the steady state entropy production is the same as a diffusive particle with constant drift v, because the RTP can be regarded as a diffusive particle with drift v ceaselessly changing direction instantaneously, and these instant changes of direction will not produce entropy [41]. Thus, it is obvious from Eq. (10) that the TUR (9) is validated. Then a transport efficiency

$$\eta_\tau \equiv \frac{\Sigma_{\mathrm{TUR}}^\tau}{\langle \Sigma \rangle} = \frac{\left(\gamma_l^2 - \gamma_r^2\right)^2}{\frac{D_{\mathrm{eff}}}{2D}\left(\frac{\gamma_r+\gamma_l}{\gamma_r-\gamma_l}\right)^2 - \frac{8\gamma_l\gamma_r v^2[1-e^{-(\gamma_l+\gamma_r)\tau}]}{2\left(\gamma_l^2-\gamma_r^2\right)^2 D\tau}} \leqslant 1 \tag{11}$$

can be defined to evaluate the efficiency of estimation [31,42]. To illustrate the estimating effect of TUR, we plot the transport efficiency from TUR with different observation time τ and different activity v in Fig. 2.

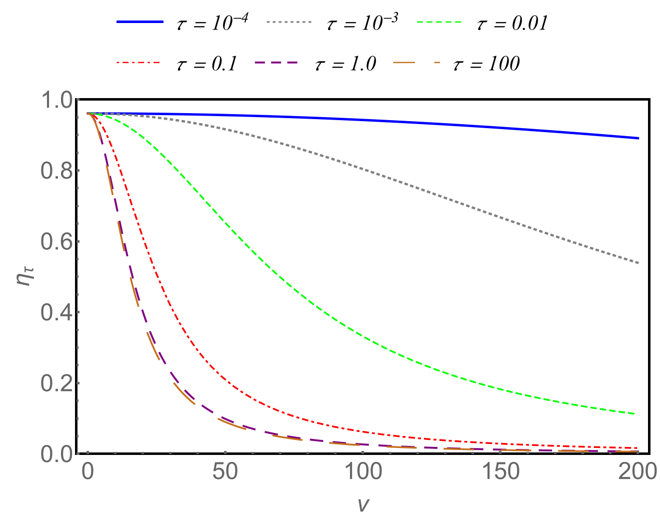

FIG. 2. The transport efficiency η_τ from the TUR bound versus the activity v with different observation times τ. The model parameters are chosen as $\gamma_l = 10,\ \gamma_r = 0.1,\ D = 1.0$.

From the above expression and plot we can draw some conclusions. First, if the drift velocity v is very large, i.e., the

RTP is far from equilibrium, and meanwhile the observation time τ is large for experimental convenience, then the TUR bound will become very loose and therefore cannot work well for the entropy production estimation, whatever other system details are. It has been reported that the TUR can be tight in the linear-response regime, but generally it will be loose when the system is far from equilibrium [26,27,37]. Physically, this is because of the presence of excess fluctuations (quantified by high-order cumulants) far from equilibrium [38]. In the linear-response regime these fluctuations are negligible so that the TUR can be tight. Second, in the short observation time limit ($\tau \to 0$) the TUR estimator would work remarkably well compared to the large observation time cases:

$$\lim_{\tau\to\infty} \eta_\tau = \frac{2D}{D_{\text{eff}}}\left(\frac{\gamma_r-\gamma_l}{\gamma_r+\gamma_l}\right)^2 \leqslant \lim_{\tau\to 0} \eta_\tau = \left(\frac{\gamma_r-\gamma_l}{\gamma_r+\gamma_l}\right)^2 \leqslant 1, \tag{12}$$

whose estimating effect would be robust even in the far from equilibrium region ($v \gg 1$), since it is irrelevant to the drift velocity v. The inequality saturates when $\gamma_r = 0$, i.e., the particle won't tumble, but always move forward with a constant mean velocity. When $\gamma_r = \gamma_l$, TUR becomes trivial and cannot gives any prediction, because the mean displacement vanishes, making the TUR estimator vanish as well. The robustness under activity is in fact the advantage of the recently found short-time TUR [34,43]. The short-time TUR is tight even in the far from equilibrium regime, for the reason that the short observation time kills excess fluctuations (interested readers can refer to Supplemental Material of [34] for details). However, experimental scientists may prefer large measurement time TUR as an estimating method, due to the limitation of time resolution of common tools. Here we would like to address this issue utilizing the HTUR.

IV. HIGH-ORDER THERMODYNAMIC UNCERTAINTY RELATION AND ITS APPLICATION TO ESTIMATE ENTROPY PRODUCTION

Recently, Dechant and Sasa [36] constructed a HTUR from their fluctuation-response inequality in both Langevin systems and discrete-state Markov systems, which reads

$$\langle x_\tau\rangle^2 \sup_h F(h) \leqslant \langle \Sigma_\tau\rangle,$$

$$F(h) := \frac{h^2}{K_{x_\tau}(h) - h\langle x_\tau\rangle}, \tag{13}$$

where $K_{x_\tau}(h) \equiv \ln\langle e^{hx_\tau}\rangle$ is the CGF of the current x_τ (this inequality works for generalized current j_τ; in this work we only focus on x_τ). The conventional TUR can be readily recovered from Eq. (13) by taking the $h \to 0$ limit. It has been demonstrated that, in a general jump-diffusion model [36], Eq. (13) still works (see Appendix C for details). This type of process can be described by the equation

$$\dot{x}(t) = a_{k(t)}[x(t)] + \sqrt{2D_{k(t)}}\xi(t), \tag{14}$$

where the drift term $a_{k(t)}[x(t)]$ and diffusion coefficient $D_{k(t)}$ can jump between multiple discrete states $k = 1, \ldots, N$. The jumping dynamics is described by a Markov jump process with transition rates W_{ij} from state j to state i. This model covers our RTP as a specific case, thus the HTUR can be applied to our model.

To enhance the estimation of entropy production on account of HTUR, we calculate the CGF of the current x_τ below. We define some quantities for later use:

$$\langle e^{hx(\tau)}\rangle_r \equiv \int e^{hx} p_r(x,\tau)dx, \tag{15}$$

$$\langle e^{hx(\tau)}\rangle_l \equiv \int e^{hx} p_l(x,\tau)dx, \tag{16}$$

so that

$$\langle e^{hx(\tau)}\rangle = \langle e^{hx(\tau)}\rangle_r + \langle e^{hx(\tau)}\rangle_l. \tag{17}$$

It can be readily demonstrated that (see Appendix D for proof)

$$\langle e^{hx_\tau}\rangle = \langle e^{hx(\tau)}\rangle_{x(0)=0}, \tag{18}$$

which is in accordance with physical intuition since the initial position $x(0)$ is extracted from the uniform steady state distribution (any two points in our stationary system are identical). Then one can directly write down the evolution equations for $\langle e^{hx(\tau)}\rangle_{r,l}$ by multiplying e^{hx} on both sides of the Fokker-Planck equations (4) and (5) and integrating over the whole range of x, i.e.,

$$\frac{d\langle e^{hx(\tau)}\rangle_r}{d\tau} = (Dh^2 + vh - \gamma_r)\langle e^{hx(\tau)}\rangle_r + \gamma_l\langle e^{hx(\tau)}\rangle_l, \tag{19}$$

$$\frac{d\langle e^{hx(\tau)}\rangle_l}{d\tau} = (Dh^2 - vh - \gamma_l)\langle e^{hx(\tau)}\rangle_l + \gamma_r\langle e^{hx(\tau)}\rangle_r. \tag{20}$$

The above equations can be rewritten in a compact vector form

$$\frac{d\vec{\phi}(\tau)}{d\tau} = \mathcal{L}\vec{\phi}(\tau), \tag{21}$$

where

$$\vec{\phi}(\tau) \equiv (\langle e^{hx(\tau)}\rangle_r, \langle e^{hx(\tau)}\rangle_l)^{\mathrm{T}}$$

and

$$\mathcal{L} = \begin{pmatrix} Dh^2 + vh - \gamma_r & \gamma_l \\ \gamma_r & Dh^2 - vh - \gamma_l \end{pmatrix}.$$

Equation (21) is linear, thus its solution can be formally written as

$$\vec{\phi}(\tau) = e^{\mathcal{L}\tau}\vec{\phi}(0), \tag{22}$$

with the initial condition being $[x(0) = 0]$

$$\vec{\phi}(0) = \left(\frac{\gamma_l}{\gamma_l+\gamma_r}, \frac{\gamma_r}{\gamma_l+\gamma_r}\right)^{\mathrm{T}}.$$

Then the closed form of $K_{x_\tau}(h)$ can be obtained by

$$K_{x_\tau}(h) = \ln(\langle e^{hx(\tau)}\rangle_r + \langle e^{hx(\tau)}\rangle_l), \tag{23}$$

which is too lengthy to show here. We include the detailed form of it in Appendix D for completeness. However, in the short observation time limit $\tau \to 0$, the expression of the CGF is brief (high-order terms may be dropped due to their negligible effects in the maximization problem):

$$K_{x_\tau}(h) = \langle x_\tau\rangle h + Dh^2\tau + \mathcal{O}(\tau^2), \tag{24}$$

resulting in the same lower bound as the short-time TUR:

$$\Sigma_{\text{HTUR}}^{\tau\to 0} = \left(\frac{\gamma_r - \gamma_l}{\gamma_r + \gamma_l}\right)^2 \frac{v^2}{D}\tau = \frac{\langle x_\tau\rangle^2}{D\tau}. \tag{25}$$

Additionally, the leading contribution $K_{\text{lead}}(h)$ of $K_{x_\tau}(h)$ in the large τ limit could be identified as

$$\frac{2Dh^2 + \sqrt{(\gamma_l+\gamma_r)^2 - 4hv(\gamma_l-\gamma_r) + 4h^2v^2} - \gamma_l - \gamma_r}{2}\tau. \tag{26}$$

Then maximizing

$$\frac{h^2}{K_{\text{lead}}(h) - h\langle x_\tau\rangle} \tag{27}$$

over the whole range of h remarkably gives rise to $1/D\tau$, when $h\to\infty$. This still leads to the tight bound (25) as in the small τ limit. In other cases with $0<\tau<\infty$ the optimization problem $\sup_h F(h)$ from HTUR might not be solved generally when parameters are not fixed. In spite of this, we discover that for any τ the $h\to\infty$ limit for $F(h)$ can be obtained as (see Appendix D for details):

$$\lim_{h\to\infty} F(h) = \frac{1}{D\tau}, \tag{28}$$

which means that the lower bound $\Sigma_{\text{HTUR}}^{\tau}$ given by HTUR cannot be smaller than $\frac{1}{D\tau}$, because the lower bound is given by the maximal value of $F(h)$. That is, we have

$$\langle\Sigma_\tau\rangle \geqslant \Sigma_{\text{HTUR}}^{\tau} = \langle x_\tau\rangle^2 \sup_h F(h) \geqslant \frac{\langle x_\tau\rangle^2}{D\tau}. \tag{29}$$

After numerically exploring a large amount of values over the parameter space $(\gamma_l, \gamma_r, v, D, \tau)$, we claim that $F(h) = \frac{h^2}{K_{x_\tau}(h) - h\langle x_\tau\rangle}$ is an increasing function of h when $h>0$, and when $h<0$ the function $F(h) < F(-h)$ (see Appendix E for numerical evidence). Based on the above findings, we conjecture that a new lower bound for entropy production from HTUR for any observation time τ is given by

$$\Sigma_{\text{HTUR}}^{\tau} = \frac{\langle x_\tau\rangle^2}{D\tau}, \tag{30}$$

which is our main result.

Some remarks on this result can be made. First, the estimation of entropy production rate from Eq. (30) would not be affected by the variation in observation time τ, and would be robust even in the far from equilibrium region, in stark contrast to the conventional TUR. Second, when the diffusion constant D (or the friction coefficient) is known, the energy dissipation during τ can be estimated experimentally only by readily measuring the mean displacement $\langle x_\tau\rangle$ during that time interval. Therefore, the HTUR estimator may find potential application in many active matter systems, since the amount of trajectory data needed for is pretty small compared to other methods. However, because the system details are usually unknown, one would prefer to measure the dissipation only through the trajectory information, in which case the CGF should be measured to obtain our tighter bound. Notwithstanding that the CGF—which contains the information of infinite higher-order cumulants—may not be experimentally feasible, we show in Fig. 3 that when the factor h is fixed the left-hand-side of Eq. (13) can still serve as a pretty good estimator for entropy production, i.e.,

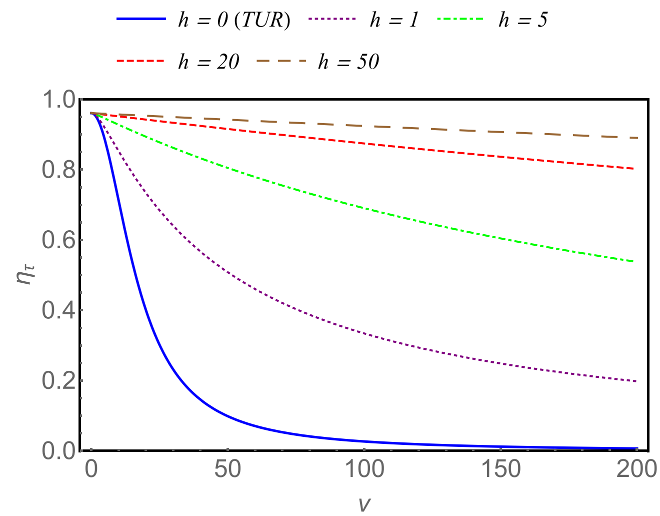

FIG. 3. The transport efficiency $\eta_\tau = \Sigma_{h=a}^{\tau}/\langle\Sigma_\tau\rangle$ from the TUR bound and from the improved bound vs the activity v with different h. The model parameters are chosen as $\gamma_l = 10,\ \gamma_r = 0.1,\ D = 1.0,\ \tau = 1.0$

$$\Sigma_{h=a}^{\tau} \equiv \frac{a^2\langle x_\tau\rangle^2}{\ln\langle e^{ax_\tau}\rangle - a\langle x_\tau\rangle} \leqslant \langle\Sigma_\tau\rangle. \tag{31}$$

And when h is fixed, the resulting estimator could be experimentally obtained from the time series data of trajectories, without prior knowledge of the model details. Strikingly, as shown in Fig. 3, even the estimator

$$\Sigma_{h=1}^{\tau} = \frac{\langle x_\tau\rangle^2}{\ln\langle e^{x_\tau}\rangle - \langle x_\tau\rangle} \tag{32}$$

in the $h=1$ case would greatly improve the estimation of entropy production compared to the conventional TUR, behaving much better in the far from equilibrium regime. When the chosen values of h are increasing, the resulting estimators become better and better, and asymptotically converge to the best one $\Sigma_{\text{HTUR}}^{\tau}$.

V. DISCUSSION

In this paper, we explore the stochastic thermodynamics of an asymmetric run-and-tumble particle, which may model behaviors of molecular motors or chemotaxis motions of some active bacteria. We first explore the finite-time TUR in our system, revealing that the short observation time strategy is beneficial for the estimation of entropy production. Most importantly, resorting to the HTUR, we have shown that an improved estimation of energy dissipation only from experimentally feasible trajectory data can be realized. The HTUR estimating strategy is robust when the RTP is arbitrarily far from equilibrium, and its effect will not be affected by the observation time τ, forming a sharp contrast to the conventional TUR. Based on the HTUR, we further propose an experimentally viable estimating strategy for entropy production rate, and check its effect through the analytical expression of

CGF, showing that the strategy still significantly outperform the conventional TUR strategy. We would like to emphasize the advantage of our estimating strategy based on TUR or HTUR. The chosen current observable can be measured on a very coarse-grained level, so that only a moderate amount of trajectory data is required. To apply our strategy, there is even no need to track the whole trajectory of the position x. For each experiment, measurements of the number of cycles the particle goes through during the observation time, the initial position, and the final position of the particle at time τ are enough for estimation, with detecting the current state of the particle (run state or tumble state) being unnecessary. To apply our estimating method, the requirement for the spatial and temporal resolution of experimental equipment is relatively low. Therefore, we reveal the potential strength of HTUR in the estimation of entropy production in active matter systems.

There are still some limitations of our work. The asymmetry of the hopping rate between run state and tumble state is necessary for our estimators both from conventional TUR and HTUR, due to the choice of displacement as the current to use. If one chooses the entropy production itself as a current, the TUR and HTUR bound can be saturated even in the symmetric case $\gamma_l = \gamma_r$ [27,34,43], in which our bound cannot be applied. Nevertheless, our aim is to estimate the entropy production of RTP; once the entropy production itself is known, there is no need to do any more estimation. Therefore, whether there is a good estimator in the symmetric case $\gamma_l = \gamma_r$ still remains an open problem, which we leave for future work. Further, when the RTP is trapped in a confined potential (see Appendix B for an example), the mean displacement vanishes in the stationary state, in which case also our estimator cannot take effect. Besides, the generalization of our method to two-dimensional RTP is nontrivial and deserves further study.

ACKNOWLEDGMENTS

This work is supported by MOST (Grant No. 2018YFA0908702) and NSFC (Grant No. 21833007).

APPENDIX A: A SIMPLE DERIVATION OF Eq. (3)

From the definition of stationary average, we directly write down

$$\langle\sigma(t)\sigma(s)\rangle = \sum_{\sigma_1,\sigma_2=\pm1} \sigma_1\sigma_2 p(\sigma_2, t|\sigma_1, s)p^{st}(\sigma_1) \tag{A1}$$

$$= \sum_{\sigma_1} \langle\sigma(t)\rangle_{\sigma_1,s}\sigma_1 p^{st}(\sigma_1), \tag{A2}$$

where $\langle\sigma(t)\rangle_{\sigma_1,s}$ is the conditional average with the initial condition being $\sigma(s) = \sigma_1$. From the Fokker-Planck equation, which $p(\sigma, t|\sigma_1, s)$ obeys, and the initial condition $p(\sigma, s|\sigma_1, s) = \delta_{\sigma,\sigma_2}$, one can solve that

$$p(\sigma = 1, t|\sigma_1, s) = \frac{\gamma_l}{\gamma_l+\gamma_r} + e^{-(\gamma_l+\gamma_r)(t-s)} \times \left(\frac{\gamma_r}{\gamma_l+\gamma_r}\delta_{1,\sigma_1} - \frac{\gamma_l}{\gamma_l+\gamma_r}\delta_{-1,\sigma_1}\right), \tag{A3}$$

$$p(\sigma = -1, t|\sigma_1, s) = \frac{\gamma_r}{\gamma_l+\gamma_r} - e^{-(\gamma_l+\gamma_r)(t-s)} \times \left(\frac{\gamma_r}{\gamma_l+\gamma_r}\delta_{1,\sigma_1} - \frac{\gamma_l}{\gamma_l+\gamma_r}\delta_{-1,\sigma_1}\right). \tag{A4}$$

Then the conditional average can be computed as

$$\langle\sigma(t)\rangle_{\sigma_1,s} = \sum_{\sigma=\pm1}\sigma(t)p(\sigma, t|\sigma_1, s) = \frac{\gamma_l-\gamma_r}{\gamma_l+\gamma_r} + e^{-(\gamma_l+\gamma_r)(t-s)}\left(\sigma_1 - \frac{\gamma_l-\gamma_r}{\gamma_l+\gamma_r}\right). \tag{A5}$$

Plugging Eq. (A5) into Eq. (A2) and using

$$p^{st}(\sigma = 1) = \frac{\gamma_l}{\gamma_l+\gamma_r},$$

$$p^{st}(\sigma = -1) = \frac{\gamma_r}{\gamma_l+\gamma_r}$$

one obtains that

$$\langle\sigma(t)\sigma(s)\rangle = \frac{4\gamma_r\gamma_l}{(\gamma_r+\gamma_l)^2}e^{-(\gamma_r+\gamma_l)|t-s|} + \left(\frac{\gamma_r-\gamma_l}{\gamma_r+\gamma_l}\right)^2, \tag{A6}$$

which is just Eq. (3) in the main text.

APPENDIX B: MOMENT EQUATIONS OF THE RUN-AND-TUMBLE PARTICLE IN ONE DIMENSION

In this Appendix, we introduce the moment equations method and give some applications.

Calculation of variance of the current x_τ

In this subsection, we use the moment equations method to obtain the variance for the one-dimensional RTP, which is useful in the main text. First we define some useful quantities. The nth right moment, left moment, and moment of the position at time t are respectively given by

$$\langle x^n\rangle_r \equiv \int x(t)^n p_r(x, t)dx,$$

$$\langle x^n\rangle_l \equiv \int x(t)^n p_l(x, t)dx,$$

$$\langle x^n\rangle = \langle x^n\rangle_r + \langle x^n\rangle_l = \int x(t)^n p(x, t)dx. \tag{B1}$$

Multiplying x^n on both sides of Eqs. (4) and (5), one obtains the evolution equations for the nth right moment and left moment as

$$\frac{d\langle x^n\rangle_r}{dt} = \theta_{n,1}nv\langle x^{n-1}\rangle_r + \theta_{n,2}Dn(n-1)\langle x^{n-2}\rangle_r - \gamma_r\langle x^n\rangle_r + \gamma_l\langle x^n\rangle_l, \tag{B2}$$

$$\frac{d\langle x^n\rangle_l}{dt} = -\theta_{n,1}nv\langle x^{n-1}\rangle_l + \theta_{n,2}Dn(n-1)\langle x^{n-2}\rangle_r + \gamma_r\langle x^n\rangle_r - \gamma_l\langle x^n\rangle_l, \tag{B3}$$

where $\theta_{n,c}$ equals 1 for $n \geqslant c$ and 0 for $n < c$. When $n = 0$, the above equations reduce to

$$\frac{d\langle x^0\rangle_r}{dt} = -\gamma_r\langle x^0\rangle_r + \gamma_l\langle x^0\rangle_l, \tag{B4}$$

$$\frac{d\langle x^0\rangle_l}{dt} = \gamma_r\langle x^0\rangle_r - \gamma_l\langle x^0\rangle_l. \tag{B5}$$

In the large time limit that we are interested in, combining Eq. (B4) and (B5) with the conservation of probability $\langle x^0\rangle_r + \langle x^0\rangle_l = 1$ gives rise to $\langle x^0\rangle_r = \gamma_l/(\gamma_l+\gamma_r)$ and $\langle x^0\rangle_l = \gamma_r/(\gamma_l+\gamma_r)$. When $n = 1$, the first-order moment equations are

$$\frac{d\langle x\rangle_r}{dt} = v\frac{\gamma_l}{\gamma_l+\gamma_r} - \gamma_r\langle x\rangle_r + \gamma_l\langle x\rangle_l, \tag{B6}$$

$$\frac{d\langle x\rangle_l}{dt} = -v\frac{\gamma_r}{\gamma_l+\gamma_r} + \gamma_r\langle x\rangle_r - \gamma_l\langle x\rangle_l, \tag{B7}$$

which leads to

$$\frac{d\langle x\rangle}{dt} = \frac{d\langle x\rangle_r}{dt} + \frac{d\langle x\rangle_l}{dt} = v\frac{\gamma_l-\gamma_r}{\gamma_l+\gamma_r}. \tag{B8}$$

From the initial condition $\langle x(0)\rangle = \langle x\rangle^{st} = L/2$, the first moment at time τ is yielded:

$$\langle x(\tau)\rangle = \langle x\rangle_r + \langle x\rangle_l = v\frac{\gamma_l-\gamma_r}{\gamma_l+\gamma_r}\tau + \frac{L}{2}, \tag{B9}$$

Combining Eq. (B9) with the first-order equations, the first left and right moments at time τ can also be expressed as

$$\langle x\rangle_r = \frac{\gamma_l L}{2(\gamma_l+\gamma_r)} + \frac{\gamma_l\big[(\gamma_l^2-\gamma_r^2)\tau + 2\gamma_r\big]v}{(\gamma_l+\gamma_r)^3} - \frac{2\gamma_l\gamma_r v e^{-(\gamma_l+\gamma_r)\tau}}{(\gamma_l+\gamma_r)^3}, \tag{B10}$$

$$\langle x\rangle_l = \frac{\gamma_r L}{2(\gamma_l+\gamma_r)} + \frac{\gamma_r\big[(\gamma_l^2-\gamma_r^2)\tau - 2\gamma_l\big]v}{(\gamma_l+\gamma_r)^3} + \frac{2\gamma_l\gamma_r v e^{-(\gamma_l+\gamma_r)\tau}}{(\gamma_l+\gamma_r)^3}, \tag{B11}$$

having taken the initial conditions (steady state)

$$\langle x_0\rangle_r = \frac{L}{2}\frac{\gamma_l}{\gamma_l+\gamma_r}, \quad \langle x_0\rangle_l = \frac{L}{2}\frac{\gamma_r}{\gamma_l+\gamma_r} \tag{B12}$$

into account. Then from the second-order moment equations ($n = 2$), one can figure out the variance of $x(\tau)$, which reads

$$\frac{d\langle x^2\rangle_r}{dt} = 2v\langle x\rangle_r + 2D\langle x^0\rangle_r - \gamma_r\langle x^2\rangle_r + \gamma_l\langle x^2\rangle_l, \tag{B13}$$

$$\frac{d\langle x^2\rangle_l}{dt} = -2v\langle x\rangle_l + 2D\langle x^0\rangle_l + \gamma_r\langle x^2\rangle_r - \gamma_l\langle x^2\rangle_l. \tag{B14}$$

Thus the second moment of $x(\tau)$ arises from the equation

$$\frac{d\langle x^2\rangle}{dt} = 2v(\langle x\rangle_r - \langle x\rangle_l) + 2D, \tag{B15}$$

whose solution is

$$\langle x(\tau)^2\rangle = \left(\langle x(\tau)\rangle^2 - \frac{L^2}{4}\right) + D_{\mathrm{eff}}\tau - \frac{8\gamma_l\gamma_r v^2}{(\gamma_l+\gamma_r)^4}[1 - e^{-(\gamma_l+\gamma_r)\tau}] + \frac{L^2}{3} \tag{B16}$$

with the initial condition being $\langle x(0)^2\rangle = L^2/3$ and using Eqs. (B10) and (B11). Here, the effective diffusion coefficient has been defined in Eq. (8) of main text as

$$D_{\mathrm{eff}} = \frac{8\gamma_l\gamma_r v^2}{(\gamma_l+\gamma_r)^3} + 2D.$$

So the variance of $x(\tau)$ is simply

$$\mathrm{Var}(x(\tau)) = \langle x(\tau)^2\rangle - \langle x(\tau)\rangle^2 = D_{\mathrm{eff}}\tau - \frac{8\gamma_l\gamma_r v^2}{(\gamma_l+\gamma_r)^4}[1 - e^{-(\gamma_l+\gamma_r)\tau}] + \frac{L^2}{12}. \tag{B17}$$

In the stationary state, the variance of the current x_τ with observation time τ is connected to the variance of $x(\tau)$ as

$$\begin{aligned}\mathrm{Var}(x_\tau) &= \langle [x(\tau) - x(0)]^2\rangle - [\langle x(\tau)\rangle - \langle x(0)\rangle]^2 \\ &= \langle x(\tau)^2\rangle + \langle x(0)^2\rangle - 2\langle x(\tau)x(0)\rangle - \langle x(\tau)\rangle^2 \\ &\quad - \langle x(0)\rangle^2 + 2\langle x(\tau)\rangle\langle x(0)\rangle \\ &= \mathrm{Var}[x(\tau)] + L^2/12 - 2\mathrm{Cov}[x(\tau), x(0)],\end{aligned} \tag{B18}$$

where $\mathrm{Var}[x(0)] = L^2/3 - (L/2)^2 = L^2/12$ was used. Now we compute the quantity $\mathrm{Cov}[x(\tau), x(0)] = \langle x(\tau)x(0)\rangle - \langle x(\tau)\rangle\langle x(0)\rangle$. Note that

$$\langle x(\tau)x(0)\rangle = \int dx \int_0^L dx_0 x(\tau)x_0 p(x,\tau|x_0,0)p^{st}(x_0)dx\,dx_0 \tag{B19}$$

$$= \frac{1}{L}\int_0^L \langle x(\tau)\rangle_{x_0} x_0 dx_0, \tag{B20}$$

with $\langle x(\tau)\rangle_{x_0} \equiv \int x(\tau)p(x,\tau|x_0,0)dx$. According to Eq. (B8),

$$\langle x(\tau)\rangle_{x_0} = v\frac{\gamma_l-\gamma_r}{\gamma_l+\gamma_r}\tau + x_0, \tag{B21}$$

so that

$$\begin{aligned}\langle x(\tau)x(0)\rangle - \langle x(\tau)\rangle\langle x(0)\rangle &= \frac{1}{L}\int_0^L \langle x(\tau)\rangle_{x_0} x_0 dx_0 \\ &\quad - \frac{v\tau L}{2}\frac{\gamma_l-\gamma_r}{\gamma_l+\gamma_r} - \frac{L^2}{4} \\ &= \frac{L^2}{12}.\end{aligned} \tag{B22}$$

Therefore, the variance of the current x_τ is finally obtained as

$$\begin{aligned}\mathrm{Var}(x_\tau) &= \mathrm{Var}[x(\tau)] + L^2/12 - 2\mathrm{Cov}[x(\tau), x(0)] \\ &= \mathrm{Var}[x(\tau)] - \frac{L^2}{12} \\ &= D_{\mathrm{eff}}\tau - \frac{8\gamma_l\gamma_r v^2}{(\gamma_l+\gamma_r)^4}[1 - e^{-(\gamma_l+\gamma_r)\tau}],\end{aligned} \tag{B23}$$

which is just Eq. (8) of the main text. Note that the expression of moments of x_τ is irrelevant to the system size L, thus it can also be applied to the natural boundary condition case. It should be mentioned that this result can also be directly derived from the two-time correlation function of the velocity $\dot{x}(t) = v\sigma(t) + \sqrt{2D}\xi(t)$, using the celebrated Green-Kubo (G-K) formula. We sketch the derivation using the G-K formula below. Since

$$\left\langle x_\tau^2 \right\rangle = \left\langle \int_0^\tau \int_0^\tau \dot{x}(t)\dot{x}(s) ds dt \right\rangle = \int_0^\tau \int_0^\tau \langle \dot{x}(t)\dot{x}(s)\rangle ds\, dt, \tag{B24}$$

what we need to compute is the two-time correlation function

$$\begin{aligned} C(t-s) &\equiv \langle \dot{x}(t)\dot{x}(s)\rangle = v^2\langle\sigma(t)\sigma(s)\rangle + 2D\langle\xi(t)\xi(s)\rangle \\ &= v^2\left[\frac{4\gamma_r\gamma_l}{(\gamma_r+\gamma_l)^2} e^{-(\gamma_r+\gamma_l)|t-s|} + \left(\frac{\gamma_r-\gamma_l}{\gamma_r+\gamma_l}\right)^2\right] \\ &\quad + 2D\delta(t-s). \end{aligned} \tag{B25}$$

Then, according to the G-K formula,

$$\begin{aligned} \left\langle x_\tau^2 \right\rangle &= \int_0^\tau \int_0^\tau C(t-s) ds\, dt = 2\int_0^\tau C(t)(\tau - t) dt \\ &= D_{\mathrm{eff}}\tau - \frac{8\gamma_l\gamma_r v^2}{(\gamma_l+\gamma_r)^4}\left[1 - e^{-(\gamma_l+\gamma_r)\tau}\right] + \langle x_\tau\rangle^2, \end{aligned} \tag{B26}$$

so that

$$\mathrm{Var}(x_\tau) = D_{\mathrm{eff}}\tau - \frac{8\gamma_l\gamma_r v^2}{(\gamma_l+\gamma_r)^4}\left[1 - e^{-(\gamma_l+\gamma_r)\tau}\right].$$

Note that the integration of the delta function $\int_0^\tau \delta(t)dt = 1/2$ here because the Stratonovich convention is taken.

Energy dissipation rate of a RTP in a harmonic potential well

Here, we discuss another application of the moment equations method, calculating the entropy production rate of a RTP confined in a harmonic potential $U(x) = \frac{1}{2}kx^2$. The result is a slight generalization of what was obtained in Ref. [44], where the entropy production rate of a symmetric RTP in a harmonic potential was calculated through the field-theoretical method. The corresponding Langevin equation and Fokker-Planck equations are

$$\dot{x}(t) = -kx + v\sigma(t) + \sqrt{2D}\xi(t) \tag{B27}$$

and

$$\begin{aligned} \frac{\partial p_r(x,t)}{\partial t} &= \partial_x[kx - v_0 + D\partial_x]p_r(x,t) \\ &\quad - \gamma_r p_r(x,t) + \gamma_l p_l(x,t), \end{aligned} \tag{B28}$$

$$\begin{aligned} \frac{\partial p_l(x,t)}{\partial t} &= \partial_x[kx + v_0 + D\partial_x]p_l(x,t) \\ &\quad + \gamma_r p_r(x,t) - \gamma_l p_l(x,t). \end{aligned} \tag{B29}$$

In this case, the RTP will finally converge to a nonequilibrium stationary state (NESS). The moment equations at this stationary state are obtained as

$$\begin{aligned} nk\langle x^n\rangle_r &= \theta_{n,1} nv\langle x^{n-1}\rangle_r + \theta_{n,2}Dn(n-1)\langle x^{n-2}\rangle_r \\ &\quad - \gamma_r\langle x^n\rangle_r + \gamma_l\langle x^n\rangle_l, \end{aligned} \tag{B30}$$

$$\begin{aligned} nk\langle x^n\rangle_l &= -\theta_{n,1} nv\langle x^{n-1}\rangle_l + \theta_{n,2}Dn(n-1)\langle x^{n-2}\rangle_r \\ &\quad + \gamma_r\langle x^n\rangle_r - \gamma_l\langle x^n\rangle_l, \end{aligned} \tag{B31}$$

where $\langle\cdot\rangle_{r,l} = \int dx(\cdot)p_{r,l}^{st}(x)$ is the stationary state average. Note that the energy dissipation rate at the NESS is only contributed by the switching between run state and tumble state, which can be regarded as a potential switching process [25] between the left potential $V_l(x) \equiv U(x) + vx$ and the right potential $V_r(x) \equiv U(x) - vx$. Consequently, the energy dissipation rate can be readily computed by

$$\begin{aligned} W &= \int dx\, \gamma_r p_r^{st}(x)\Delta V + \int dx\, \gamma_l p_l^{st}(x)(-\Delta V) \\ &= \int dx\left[\gamma_r p_r^{st}(x) - \gamma_l p_l^{st}(x)\right][V_l(x) - V_r(x)] \\ &= 2v\int dx\left[\gamma_r p_r^{st}(x) - \gamma_l p_l^{st}(x)\right]x \\ &= 2v[\gamma_r\langle x\rangle_r - \gamma_l\langle x\rangle_l], \end{aligned} \tag{B32}$$

with $\Delta V \equiv V_l(x) - V_r(x) = 2vx$. This is because, in the presence of a confined potential, the contribution from the drift vanishes in the stationary state (effective equilibrium). From the conservation of probability $\langle x^0\rangle_r + \langle x^0\rangle_l = 1$ we still have $\langle x^0\rangle_r = \gamma_l/(\gamma_l+\gamma_r)$ and $\langle x^0\rangle_l = \gamma_r/(\gamma_l+\gamma_r)$; then taking $n = 1$ in the above stationary state moment equations brings about

$$k\langle x\rangle_r = \frac{v\gamma_l}{\gamma_l+\gamma_r} - \gamma_r\langle x\rangle_r + \gamma_l\langle x\rangle_l, \tag{B33}$$

$$k\langle x\rangle_l = \frac{-v\gamma_r}{\gamma_l+\gamma_r} + \gamma_r\langle x\rangle_r - \gamma_l\langle x\rangle_l. \tag{B34}$$

These two equations directly lead to

$$\begin{aligned} \langle x\rangle &= \langle x\rangle_r + \langle x\rangle_l = \frac{\gamma_l-\gamma_r}{\gamma_l+\gamma_r}\frac{v}{k}, \\ \langle x\rangle_r &= \frac{\gamma_l}{\gamma_l+\gamma_r+k}\left(\langle x\rangle + \frac{v}{\gamma_l+\gamma_r}\right), \\ \langle x\rangle_l &= \frac{\gamma_r}{\gamma_l+\gamma_r+k}\left(\langle x\rangle - \frac{v}{\gamma_l+\gamma_r}\right). \end{aligned} \tag{B35}$$

As a result, the steady state energy dissipation rate is

$$W = 2v[\gamma_r\langle x\rangle_r - \gamma_l\langle x\rangle_l] = \frac{4v^2\gamma_r\gamma_l}{(\gamma_l+\gamma_r+k)(\gamma_l+\gamma_r)} \tag{B36}$$

and the entropy production rate is $(D = T)$

$$\dot{\Sigma} = \frac{W}{D} = \frac{4v^2\gamma_r\gamma_l}{D(\gamma_l+\gamma_r+k)(\gamma_l+\gamma_r)}, \tag{B37}$$

reducing to the main result in Ref. [44],

$$\dot{\Sigma}_{\mathrm{sym}} = \frac{v^2\alpha}{D(k+\alpha)} \tag{B38}$$

when $\gamma_l = \gamma_r = \frac{\alpha}{2}$. In the $k \to 0$ limit,

$$\lim_{k\to 0}\dot{\Sigma} = \frac{4v^2\gamma_r\gamma_l}{D(\gamma_l+\gamma_r)^2}, \tag{B39}$$

which seems to deviate from the real entropy production rate $\frac{v^2}{D}$ when there is no confined potential (i.e., when k rigorously equals zero). Actually, there is a part of entropy production rate which is contributed by the nonzero steady state mean velocity ($\bar{v} = \frac{\gamma_l-\gamma_r}{\gamma_l+\gamma_r}v$):

$$\begin{aligned}\dot{\Sigma}_{\mathrm{v}} &= \left(p_r^{st}F_r\cdot\bar{v} + p_l^{st}F_l\cdot\bar{v}\right)\frac{1}{D}\\ &= \frac{\gamma_l-\gamma_r}{\gamma_l+\gamma_r}\frac{v}{D}\left(\frac{\gamma_l v}{\gamma_l+\gamma_r} + \frac{\gamma_r(-v)}{\gamma_l+\gamma_r}\right)\\ &= \left(\frac{\gamma_l-\gamma_r}{\gamma_l+\gamma_r}\right)^2\frac{v^2}{D},\end{aligned} \tag{B40}$$

where $F_r \equiv v$ and $F_l = -v$ are two constant forces applied to the RTP with opposite directions. Only when no confined potential exists will this part of the contribution emerge. When k is not exactly equal to zero, the particle will still be confined in a harmonic potential so that $\bar{v} = 0$ and the contribution $\dot{\Sigma}_{\mathrm{v}}$ vanishes. Adding this contribution to Eq. (B39), the real entropy production rate without confined potential is recovered:

$$\dot{\Sigma} = \frac{v^2}{D}\left[\frac{4\gamma_r\gamma_l}{(\gamma_l+\gamma_r)^2} + \left(\frac{\gamma_l-\gamma_r}{\gamma_l+\gamma_r}\right)^2\right] = \frac{v^2}{D}. \tag{B41}$$

In contrast, no matter how small the value of k is (no matter how soft the confined potential is), the mean velocity of the RTP in the stationary state vanishes once there is a confined potential. From the above analysis, we can identify the term

$$\dot{\Sigma}_{\mathrm{sw}} \equiv \frac{4v^2\gamma_r\gamma_l}{D(\gamma_l+\gamma_r)^2} \tag{B42}$$

as the part of entropy production rate originating from state switching, which may not be experimentally estimated by trajectory data using TUR or HTUR. That is, though the entropy production rate can be calculated exactly, it may be difficult to measure it experimentally without knowing the model details. Therefore, it is still an open problem to find an experimentally feasible strategy to estimate the entropy production of a RTP in a confined potential.

APPENDIX C: HIGH-ORDER TUR IN THE JUMP-DIFFUSION MODEL

In this Appendix, we derive the inequality (13) for the jump-diffusion model (14) for completeness, following Ref. [36,38]. Note that throughout this Appendix we are only focused on steady states. First, one needs to introduce a family of dynamics denoted by a parameter θ:

$$\dot{x}(t) = a^{\theta}_{k(t)}[x(t)] + \sqrt{2D_{k(t)}}\xi(t) \tag{C1}$$

with

$$a^{\theta}_{k(t)}[x(t)] = \theta v^{st}(x) + D_{k(t)}\partial_x \ln p^{st}(x). \tag{C2}$$

The $\theta \in [-1, 1]$ is called the continuous time-reversal parameter, affecting the mean current as

$$\langle J_\tau\rangle^{\theta} = \theta\langle J_\tau\rangle, \tag{C3}$$

where J_τ is the generalized current defined in Eq. (6) of the main text, and $\langle\cdot\rangle^{\theta} = \int dx(\cdot)p^{\theta}(x)$. Furthermore, the stationary state distribution $p^{st}(x)$ always remains unchanged when the value of θ changes. Considering two (path) probability densities $p^{\theta_1}(x)$ and $p^{\theta_2}(x)$ from different dynamics (here x may denote a fluctuating trajectory $\{x(t)\}_{t\in[0,\tau]}$ from 0 to τ or simply a state variable), one has

$$\begin{aligned}K^{\theta_1}_{J_\tau}(h) &= \ln\left(\int dx\, e^{hJ_\tau(x)}p^{\theta_1}(x)\right)\\ &= \ln\left(\int dx\, e^{hJ_\tau(x)}\frac{p^{\theta_1}(x)}{p^{\theta_2}(x)}p^{\theta_2}(x)\right).\end{aligned} \tag{C4}$$

Then from the concavity of the logarithm, the Jensen inequality tells us that

$$\begin{aligned}K^{\theta_1}_{J_\tau}(h) &\geqslant \int dx \ln\left(e^{hJ_\tau(x)}\frac{p^{\theta_1}(x)}{p^{\theta_2}(x)}\right)p^{\theta_2}(x)\\ &= h\langle J_\tau\rangle^{\theta_2} - D_{\mathrm{KL}}(p^{\theta_2}||p^{\theta_1}),\end{aligned} \tag{C5}$$

with the Kullback-Leibler (KL) divergence being defined as

$$D_{\mathrm{KL}}(p^{\theta_2}||p^{\theta_1}) = \int dx\, p^{\theta_2}(x)\ln\frac{p^{\theta_2}(x)}{p^{\theta_1}(x)}. \tag{C6}$$

Since inequality (C5) holds for any real value of h, it can be rewritten as a lower bound for KL divergence, which reads

$$D_{\mathrm{KL}}(p^{\theta_2}||p^{\theta_1}) \geqslant \sup_h\left[h\langle J_\tau\rangle^{\theta_2} - K^{\theta_1}_{J_\tau}(h)\right]. \tag{C7}$$

For the jump-diffusion dynamics, the KL divergence between the distributions of two dynamics can be decomposed as

$$\begin{aligned}D_{\mathrm{KL}}(p^{\theta_2}||p^{\theta_1}) &= D^{\mathrm{diff}}_{\mathrm{KL}}(p^{\theta_2}||p^{\theta_1}) + D^{\mathrm{jump}}_{\mathrm{KL}}(p^{\theta_2}||p^{\theta_1})\\ &\quad + D^{\mathrm{ini}}_{\mathrm{KL}}(p^{\theta_2}_0||p^{\theta_1}_0),\end{aligned} \tag{C8}$$

where the first term is the contribution from the diffusion part, the second term is from jump part, and the last term is from the difference in two initial distributions. Because we are considering the steady state, which is not affected by θ, the last term vanishes. It has been shown that, for path probability densities,

$$D^{\mathrm{diff}}_{\mathrm{KL}}(p^{\theta_2}||p^{\theta_1}) = \frac{(\theta_1-\theta_2)^2}{4}\langle\Sigma^{\mathrm{diff}}_\tau\rangle, \tag{C9}$$

$$D^{\mathrm{jump}}_{\mathrm{KL}}(p^{\theta_2}||p^{\theta_1}) \leqslant \frac{(\theta_1-\theta_2)^2}{4}\langle\Sigma^{\mathrm{jump}}_\tau\rangle. \tag{C10}$$

As a consequence, one has

$$\begin{aligned}D_{\mathrm{KL}}(p^{\theta_2}||p^{\theta_1}) &\leqslant \frac{(\theta_1-\theta_2)^2}{4}\left(\langle\Sigma^{\mathrm{diff}}_\tau\rangle + \langle\Sigma^{\mathrm{jump}}_\tau\rangle\right)\\ &= \frac{(\theta_1-\theta_2)^2}{4}\langle\Sigma_\tau\rangle.\end{aligned} \tag{C11}$$

Combining Eqs. (C5) and (C11) gives rise to

$$K^{\theta_1}_{J_\tau}(h) \geqslant h\theta_2\langle J_\tau\rangle - \frac{(\theta_1-\theta_2)^2}{4}\langle\Sigma_\tau\rangle. \tag{C12}$$

Then we maximize the right-hand side with respect to θ_2 resulting in a quadratic bound under any θ_1:

$$K^{\theta_1}_{J_\tau}(h) \geqslant h\theta_1\langle J_\tau\rangle + \frac{h^2\langle J_\tau\rangle^2}{\langle\Sigma_\tau\rangle}. \tag{C13}$$

Rearranging this, setting $\theta = 1$ and maximizing over the whole range of h, one obtains the HTUR (13)

$$\langle\Sigma_\tau\rangle \geqslant \langle J_\tau\rangle^2 \sup_h \frac{h^2}{K_{J_\tau}(h) - h\langle J_\tau\rangle}. \tag{C14}$$

APPENDIX D: CALCULATION OF $K_{x_\tau}(h)$ AND $\lim_{h\to\infty} F(h)$

In this Appendix, we analytically calculate the cumulant generating function $K_{x_\tau}(h) = \ln\langle e^{hx_\tau}\rangle$ of the current x_τ. First we prove the equality (18) in the main text. Denoting $x(0) = x_0$, the left-hand side of it is

$$\begin{aligned}\langle e^{hx_\tau}\rangle &= \langle e^{h[x(\tau)-x_0]}\rangle\\ &= \int dx \int_0^L dx_0 e^{h[x(\tau)-x_0]} p(x,\tau|x_0,0)p(x_0) \qquad \text{(D1)}\\ &= \int dx\, e^{hx(\tau)} p(x,\tau|x_0,0) \int_0^L e^{-hx_0} dx_0/L \qquad \text{(D2)}\\ &\equiv \frac{1}{L}\int_0^L \langle e^{hx(\tau)}\rangle_{x_0} e^{-hx_0} dx_0. \qquad \text{(D3)}\end{aligned}$$

From the main text we get

$$\begin{aligned}\langle e^{hx(\tau)}\rangle_{x_0} &= e^{\mathcal{L}\tau} e^{hx_0}\phi(0) = e^{hx_0}[e^{\mathcal{L}\tau}\phi(0)]\\ &= e^{hx_0}\langle e^{hx(\tau)}\rangle_{x_0=0},\end{aligned} \tag{D4}$$

so that

$$\begin{aligned}\langle e^{hx_\tau}\rangle &= \frac{1}{L}\int_0^L \langle e^{hx(\tau)}\rangle_{x_0} e^{-hx_0} dx_0\\ &= \langle e^{hx(\tau)}\rangle_{x_0=0}\left(\frac{1}{L}\int_0^L dx_0\right)\\ &= \langle e^{hx(\tau)}\rangle_{x_0=0},\end{aligned} \tag{D5}$$

which is just the equality (18) of the main text. Then using Eq. (22) we are able to figure out $K_{x_\tau}(h)$. The matrix $\mathcal{L}$ can always be diagonalized as $\mathcal{L} = X\Lambda X^{-1}$, where $\Lambda = \mathrm{diag}(\lambda_1, \lambda_2)$ and X is composed of its eigenvectors, since it has two different eigenvalues

$$\lambda_1 = \frac{a+b-\sqrt{(a-b)^2+4\gamma_l\gamma_r}}{2},$$

$$\lambda_2 = \frac{a+b+\sqrt{(a-b)^2+4\gamma_l\gamma_r}}{2},$$

where $a \equiv Dh^2 + vh - \gamma_r$ and $b \equiv Dh^2 - vh - \gamma_l$. As a result, the exponential of matrix $\mathcal{L}$ can be computed using

$$e^{\mathcal{L}\tau} = Xe^{\Lambda\tau}X^{-1} = X\begin{pmatrix} e^{\lambda_1\tau} & 0\\ 0 & e^{\lambda_2\tau}\end{pmatrix}X^{-1}, \tag{D6}$$

leading to the final expression of $K_{x_\tau}(h)$:

$$K_{x_\tau}(h) = \frac{a+b}{2}\tau + \ln\left[\cosh\left(\frac{f}{2}\tau\right) + C\sinh\left(\frac{f}{2}\tau\right)\right], \tag{D7}$$

with

$$f \equiv \frac{\sqrt{(a-b)^2+4\gamma_l\gamma_r}}{2}$$

and

$$C \equiv \frac{(a-b)(\gamma_l-\gamma_r)+4\gamma_l\gamma_r}{f(\gamma_l+\gamma_r)}.$$

From the above expression, it is clear that the CGF is an increasing function of $|h|$. We have checked the validity of Eq. (D7) by generating the first and second cumulants of x_τ utilizing

$$\frac{\partial K_{x_\tau}(h)}{\partial h}|_{h=0} = \langle x_\tau\rangle \tag{D8}$$

and

$$\frac{\partial^2 K_{x_\tau}(h)}{\partial h^2}|_{h=0} = \mathrm{Var}(x_\tau), \tag{D9}$$

which are equal to their true forms (7) and (8) in the main text.

In what follows we calculate $\lim_{h\to\infty} F(h)$. From the definition of f and C, it is clear that in the large-h limit

$$\begin{aligned}&f \sim h,\ C \sim \mathcal{O}(1)\\ &\Rightarrow \ln\left[\cosh\left(\frac{f}{2}\tau\right) + C\sinh\left(\frac{f}{2}\tau\right)\right] \sim h\end{aligned}$$

so that from the expression of $K_{x_\tau}(h)$ one can obtain

$$K_{x_\tau}(h) = D\tau h^2 + O(h) + \text{constant}, \tag{D10}$$

with $O(h)$ being some function of the order of h. Then one can readily compute $\lim_{|h|\to\infty} F(h)$ as

$$\begin{aligned}\lim_{|h|\to\infty} F(h) &= \lim_{|h|\to\infty} \frac{h^2}{K_{x_\tau}(h) - h\langle x_\tau\rangle}\\ &= \lim_{|h|\to\infty} \frac{1}{K_{x_\tau}(h)/h^2 - \langle x_\tau\rangle/h}\\ &= \lim_{|h|\to\infty} \frac{1}{D\tau + \mathcal{O}(|h|^{-1})}\\ &= \frac{1}{D\tau}.\end{aligned} \tag{D11}$$

APPENDIX E: NUMERICAL EVIDENCE OF $\sup_h F(h) = 1/(D\tau)$

The transport efficiency for the entropy production estimator $\frac{h^2\langle x_\tau\rangle^2}{\ln\langle e^{hx_\tau}\rangle - h\langle x_\tau\rangle}$ is given by

$$\eta(\tau,h) = \frac{\langle x_\tau\rangle^2}{\langle\Sigma_\tau\rangle}F(h) = D\tau\left(\frac{\gamma_l-\gamma_r}{\gamma_l+\gamma_r}\right)^2 F(h), \tag{E1}$$

thus $F(h) \propto \eta(\tau,h)$. As a result, to test the monotonicity of $F(h)$ one could focus on $\eta(\tau,h)$. We give the three-dimensional plots of $\eta(\tau,h)$ versus τ and h with different v, $\gamma_{l,r}$ and D, where the vertical axis denotes $\eta(\tau,h)$. The plots, Figs. 4 and 5, show the behaviors of $\eta(\tau,h)$ versus h and τ when $\gamma_l = 10$ and $\gamma_r = 0.1$. Below we explore another case when $\gamma_l = 5$ and $\gamma_r = 1$. Note that in the gray areas of the plots the value of $\eta(\tau,h)$ is very close to zero compared to the values of points in other areas. With this numerical evidence, we can claim that $F(h)$ is an increasing function of h when $h > 0$, and $F(h) \leqslant F(-h)$ when $h < 0$ for any observation

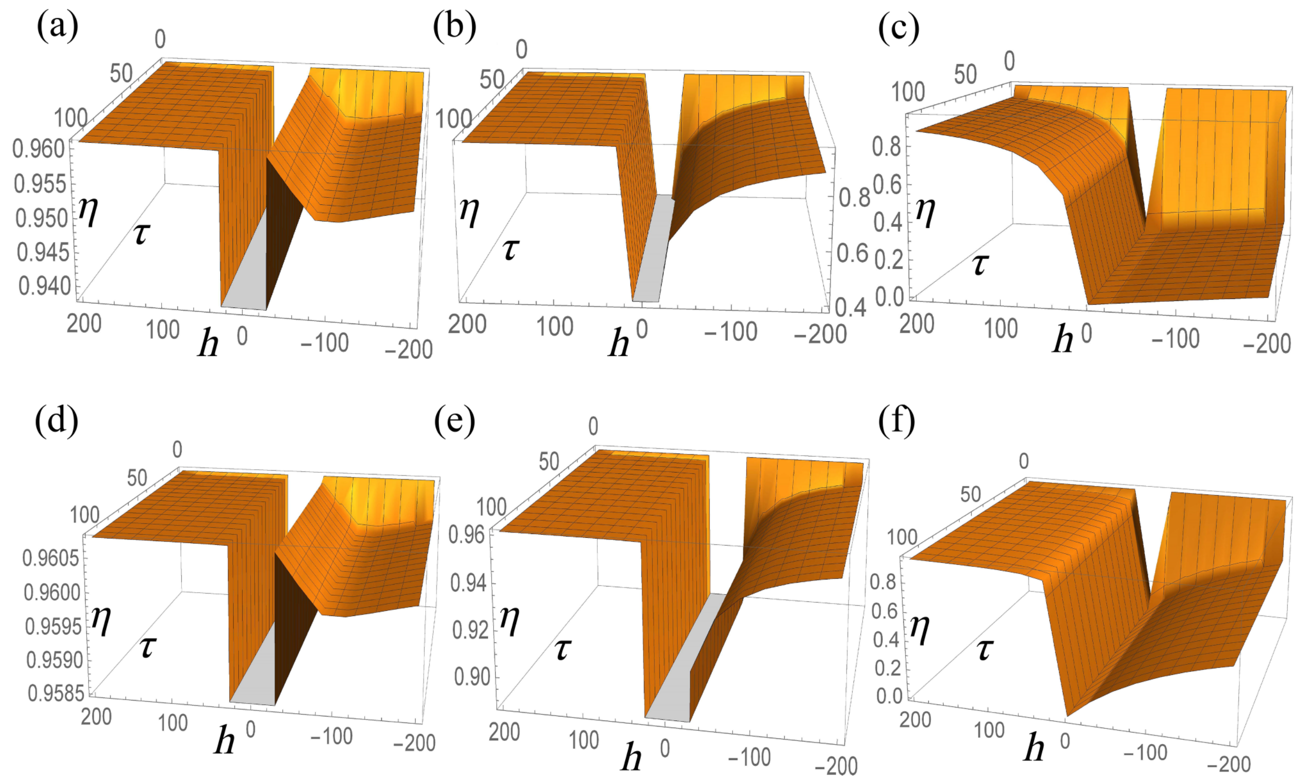

FIG. 4. The transport efficiency $\eta(\tau, h)$ vs h and τ with different D and v; transition rates are $\gamma_l = 10,\ \gamma_r = 0.1$ for this figure. For (a), (b), and (c) the parameters are chosen as $D = 1.0,\ v = 0.1,\ 1.0,\ 100$, respectively. For (d), (e), and (f) the parameters are chosen as $D = 0.1,\ v = 0.1,\ 1.0,\ 100$, respectively.

time τ, leading to the wanted result

$$\sup_h F(h) = \lim_{h\to\infty} F(h) = \frac{1}{D\tau}. \tag{E2}$$

Note that when $\gamma_l = \gamma_r$, $F(h)$ becomes a even function and $F(h) = F(-h)$; when $\gamma_l > \gamma_r$ we observe that $F(h) > F(-h)$.

We also check other cases when these parameters take other values, and no counterexample has been found.

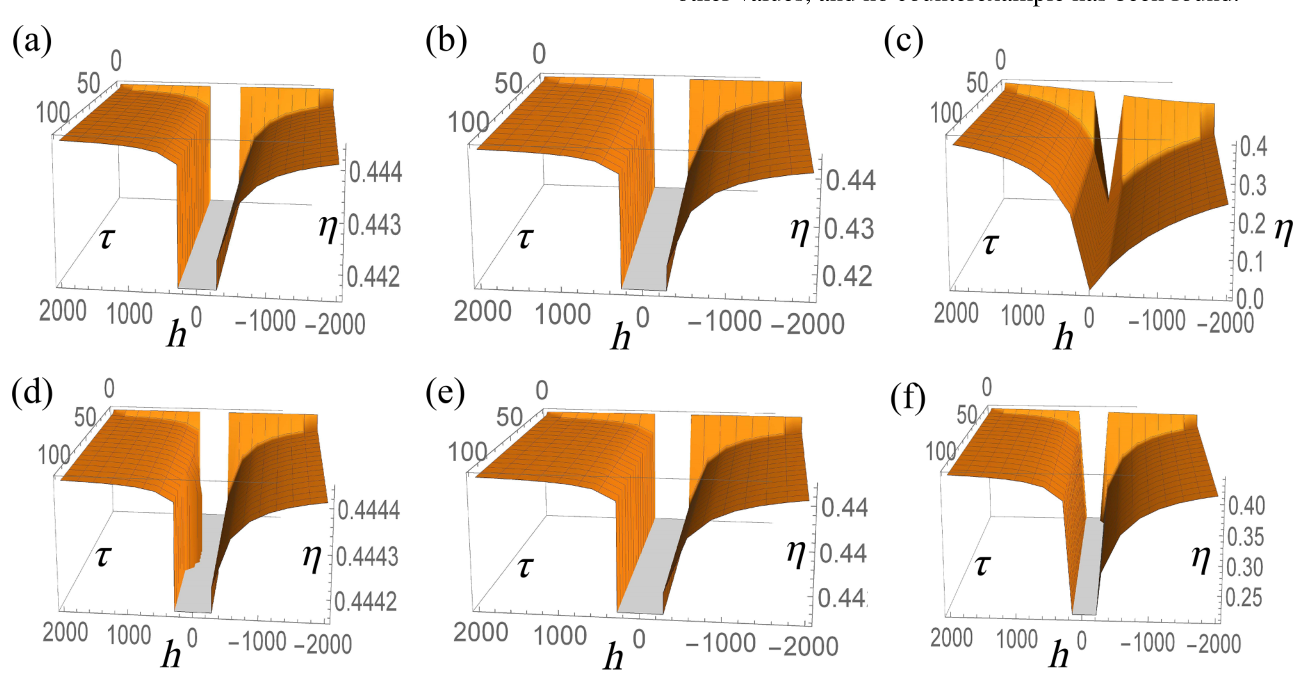

FIG. 5. The transport efficiency $\eta(\tau, h)$ vs h and τ with different D and v; transition rates are $\gamma_l = 5,\ \gamma_r = 1$ for this figure. For (a), (b), and (c) the parameters are chosen as $D = 1.0,\ v = 0.1,\ 1.0,\ 100$, respectively. For (d), (e), and (f) the parameters are chosen as $D = 0.1,\ v = 0.1,\ 1.0,\ 100$, respectively.

[1] C. Bechinger, R. Di Leonardo, H. Löwen, C. Reichhardt, G. Volpe, and G. Volpe, Rev. Mod. Phys. **88**, 045006 (2016).
[2] J. Tailleur and M. E. Cates, Phys. Rev. Lett. **100**, 218103 (2008).
[3] E. Fodor, C. Nardini, M. E. Cates, J. Tailleur, P. Visco, and F. van Wijland, Phys. Rev. Lett. **117**, 038103 (2016).
[4] L. Dabelow, S. Bo, and R. Eichhorn, Phys. Rev. X **9**, 021009 (2019).
[5] S. Shankar and M. C. Marchetti, Phys. Rev. E **98**, 020604(R) (2018).
[6] T. Vicsek, A. Czirók, E. Ben-Jacob, I. Cohen, and O. Shochet, Phys. Rev. Lett. **75**, 1226 (1995).
[7] J. Toner and Y. Tu, Phys. Rev. Lett. **75**, 4326 (1995).
[8] J. Toner and Y. Tu, Phys. Rev. E **58**, 4828 (1998).
[9] G. Szamel, Phys. Rev. E **90**, 012111 (2014).
[10] L. L. Bonilla, Phys. Rev. E **100**, 022601 (2019).
[11] G. Szamel, Phys. Rev. E **100**, 050603(R) (2019).
[12] T. Markovich and T. C. Lubensky, Phys. Rev. Lett. **127**, 048001 (2021).
[13] J. Mabillard, C. A. Weber, and F. Jülicher, Phys. Rev. E **107**, 014118 (2023).
[14] C. B. Caporusso, P. Digregorio, D. Levis, L. F. Cugliandolo, and G. Gonnella, Phys. Rev. Lett. **125**, 178004 (2020).
[15] G. Negro, C. B. Caporusso, P. Digregorio, G. Gonnella, A. Lamura, and A. Suma, Eur. Phys. J. E **45**, 75 (2022).
[16] M. Semeraro, A. Suma, I. Petrelli, F. Cagnetta, and G. Gonnella, J. Stat. Mech.: Theory Exp. (2021) 123202.
[17] D. Martin, J. O'Byrne, M. E. Cates, E. Fodor, C. Nardini, J. Tailleur, and F. van Wijland, Phys. Rev. E **103**, 032607 (2021).
[18] É. Fodor and M. Cristina Marchetti, in Lecture Notes of the 14th International Summer School on Fundamental Problems in Statistical Physics, Physica A **504**, 106 (2018).
[19] N. R. Smith, P. Le Doussal, S. N. Majumdar, and G. Schehr, Phys. Rev. E **106**, 054133 (2022).
[20] U. Basu, S. N. Majumdar, A. Rosso, and G. Schehr, Phys. Rev. E **100**, 062116 (2019).
[21] K. Malakar, A. Das, A. Kundu, K. V. Kumar, and A. Dhar, Phys. Rev. E **101**, 022610 (2020).
[22] N. Razin, Phys. Rev. E **102**, 030103(R) (2020).
[23] A. Dechant and S.-i. Sasa, Phys. Rev. X **11**, 041061 (2021).
[24] T. Harada and S.-i. Sasa, Phys. Rev. Lett. **95**, 130602 (2005).
[25] S.-W. Wang, K. Kawaguchi, S.-i. Sasa, and L.-H. Tang, Phys. Rev. Lett. **117**, 070601 (2016).
[26] A. C. Barato and U. Seifert, Phys. Rev. Lett. **114**, 158101 (2015).
[27] T. R. Gingrich, J. M. Horowitz, N. Perunov, and J. L. England, Phys. Rev. Lett. **116**, 120601 (2016).
[28] J. M. Horowitz and T. R. Gingrich, Phys. Rev. E **96**, 020103(R) (2017).
[29] P. Pietzonka, F. Ritort, and U. Seifert, Phys. Rev. E **96**, 012101 (2017).
[30] Y. Hasegawa and T. Van Vu, Phys. Rev. E **99**, 062126 (2019).
[31] A. Dechant and S.-i. Sasa, J. Stat. Mech.: Theory Exp. (2018) 063209.
[32] B. Das, S. K. Manikandan, and A. Banerjee, Phys. Rev. Res. **4**, 043080 (2022).
[33] Z. Cao and Z. Hou, J. Chem. Phys. **157**, 025102 (2022).
[34] S. K. Manikandan, D. Gupta, and S. Krishnamurthy, Phys. Rev. Lett. **124**, 120603 (2020).
[35] Z. Cao, H. Jiang, and Z. Hou, Phys. Rev. Res. **2**, 043331 (2020).
[36] A. Dechant and S.-i. Sasa, Proc. Natl. Acad. Sci. USA **117**, 6430 (2020).
[37] T. Kamijima, S. Otsubo, Y. Ashida, and T. Sagawa, Phys. Rev. E **104**, 044115 (2021).
[38] A. Dechant and S.-i. Sasa, Phys. Rev. Res. **3**, L042012 (2021).
[39] S. Ro, B. Guo, A. Shih, T. V. Phan, R. H. Austin, D. Levine, P. M. Chaikin, and S. Martiniani, Phys. Rev. Lett. **129**, 220601 (2022).
[40] U. Seifert, Rep. Prog. Phys. **75**, 126001 (2012).
[41] L. Cocconi, R. Garcia-Millan, Z. Zhen, B. Buturca, and G. Pruessner, Entropy **22**, 1252 (2020).
[42] W. Hwang and C. Hyeon, J. Phys. Chem. Lett. **9**, 513 (2018).
[43] S. Otsubo, S. Ito, A. Dechant, and T. Sagawa, Phys. Rev. E **101**, 062106 (2020).
[44] R. Garcia-Millan and G. Pruessner, J. Stat. Mech.: Theory Exp. (2021) 063203.